



**Cite this article:** Liu Y, Sun N, Hu J, Li S, Qin G. 2018 Photocatalytic degradation properties of  $\alpha$ -Fe<sub>2</sub>O<sub>3</sub> nanoparticles for dibutyl phthalate in aqueous solution system. *R. Soc. open sci.* **5**: 172196.

<http://dx.doi.org/10.1098/rsos.172196>

Received: 21 December 2017

Accepted: 13 March 2018

**Subject Category:**

Chemistry

**Subject Areas:**

green chemistry/materials science/chemical engineering

**Keywords:**

$\alpha$ -Fe<sub>2</sub>O<sub>3</sub>, nanoparticles, photocatalytic degradation, dibutyl phthalate

**Authors for correspondence:**

Jianshe Hu

e-mail: [huj@simm.neu.edu.cn](mailto:huj@simm.neu.edu.cn)

Gaowu Qin

e-mail: [qingw@simm.neu.edu.cn](mailto:qingw@simm.neu.edu.cn)

This article has been edited by the Royal Society of Chemistry, including the commissioning, peer review process and editorial aspects up to the point of acceptance.

Electronic supplementary material is available online at <https://dx.doi.org/10.6084/m9.figshare.c.4042994>.



# Photocatalytic degradation properties of $\alpha$ -Fe<sub>2</sub>O<sub>3</sub> nanoparticles for dibutyl phthalate in aqueous solution system

Yue Liu<sup>1</sup>, Nan Sun<sup>1</sup>, Jianshe Hu<sup>1</sup>, Song Li<sup>2</sup> and Gaowu Qin<sup>2</sup>

<sup>1</sup>Center for Molecular Science and Engineering, College of Science, and <sup>2</sup>School of Materials Science and Engineering, Northeastern University, Shenyang 110819, People's Republic of China

The phthalate ester compounds in industrial wastewater, as kinds of environmental toxic organic pollutants, may interfere with the body's endocrine system, resulting in great harm to humans. In this work, the photocatalytic degradation properties of dibutyl phthalate (DBP) were investigated using  $\alpha$ -Fe<sub>2</sub>O<sub>3</sub> nanoparticles and H<sub>2</sub>O<sub>2</sub> in aqueous solution system. The optimal parameters and mechanism of degradation were discussed by changing the morphology and usage amount of catalysts, the dosage of H<sub>2</sub>O<sub>2</sub>, pH value and the initial concentration of DBP. Hollow  $\alpha$ -Fe<sub>2</sub>O<sub>3</sub> nanoparticles showed the highest degradation efficiency when 30 mg of catalyst and 50  $\mu$ l of H<sub>2</sub>O<sub>2</sub> were used in the DBP solution with the initial concentration of 13 mg l<sup>-1</sup> at pH = 6.5. When the reaction time was 90 min, DBP was degraded 93% for the above optimal parameters. The photocatalytic degradation mechanism of DBP was studied by the gas chromatography–mass spectrometry technique. The result showed that the main degradation intermediates of DBP were *ortho*-phthalate monobutyl ester, methyl benzoic acid, benzoic acid, benzaldehyde, and heptyl aldehyde when the reaction time was 2 h. DBP and its intermediates were almost completely degraded to CO<sub>2</sub> and H<sub>2</sub>O in 12 h in the  $\alpha$ -Fe<sub>2</sub>O<sub>3</sub>/H<sub>2</sub>O<sub>2</sub>/UV system.

## 1. Introduction

As is well known, dibutyl phthalate (DBP) has been widely used as an excellent plasticizer in different resins, especially poly(vinyl chloride) resins and nitrocellulose [1,2]. In addition, DBP is also an important additive in special paints and adhesives. As DBP is

only physically bound to the plastic structure, it is easily released into the natural environment [3,4]. It leads to a sharp increase in the content of DBP in our living environment. However, DBP is a rather stable compound in the natural environment [5,6]. Its hydrolysis half-life is about 20 years. The people employed in the production of this plasticizer for a long time might suffer from multiple neuritis, spinal neuritis and multiple cerebral neuritis. Therefore, it is very necessary and important to study an efficient method for the degradation of DBP in wastewater.

The conventional methods, including electrochemical method [7], chemical adsorption method [8], adsorption method [9], biodegradation method [10], only transfer the organic pollutants from one phase to another, which do not degrade [11]. However, catalytic oxidation can overcome the shortcomings of these traditional methods. So the development of photocatalytic degradation technology has brought new potential for the treatment of environmental pollutants and energy crisis response. At present, the photocatalytic degradation technology has been the most active research field in waste water, waste gas purification and hydrogen production [12–15].

As an important photocatalytic material,  $\alpha$ -Fe<sub>2</sub>O<sub>3</sub> exhibits good properties [16], such as low-cost synthesis, no secondary pollution [17], n-type semiconducting behaviour and band gap ( $E_g = 2.1$  eV) [18]. It has attracted considerable attention due to its potential application in the fields of sensors, pigments, actuators, catalysts and so on [19–21].

Until now, there have been numerous reports on photocatalytic degradation of environmental pollutants by TiO<sub>2</sub> [22–24]. By contrast, there is little research on the photocatalytic degradation by Fe<sub>2</sub>O<sub>3</sub> of organic pollutants. Moreover, its corresponding reaction mechanism has not been explained in detail. Compared with those of TiO<sub>2</sub>, the valence electrons of Fe<sub>2</sub>O<sub>3</sub> can be excited by less than 560 nm to the conduction band; this can greatly improve the efficiency of the use of sunlight [25].

In previous work, we reported  $\alpha$ -Fe<sub>2</sub>O<sub>3</sub> nanoparticles with different morphologies [26]. In this study, the photocatalytic effect of  $\alpha$ -Fe<sub>2</sub>O<sub>3</sub> nanoparticles was evaluated through the degradation of DBP. The effect of the operating parameters, such as the morphology and dosage of Fe<sub>2</sub>O<sub>3</sub>, the initial concentration of H<sub>2</sub>O<sub>2</sub>, the initial concentration of DBP and the pH of solution, on the degradation efficiency was discussed. The photocatalytic reaction mechanism and degradation process of DBP over  $\alpha$ -Fe<sub>2</sub>O<sub>3</sub> were investigated with gas chromatography–mass spectrometry (GC-MS).

## 2. Experimental

### 2.1. Materials

DBP was purchased from Shenyang Li Cheng Reagent plant (Shenyang, China). Hydrogen peroxide (30%) was purchased from Shenyang Xinxing Chemical Reagent plant (Shenyang, China). The  $\alpha$ -Fe<sub>2</sub>O<sub>3</sub> nanoparticles with different morphologies were prepared in our laboratory [26]. All other solvents and reagents used were purified by standard methods.

### 2.2. Characterization

The absorption wavelength was measured by a TU-1901 dual-beam UV–visible spectrophotometer (Beijing Purkinje General Instrument Co. Ltd, China) with a range of 450–600 nm. The degradation products of DBP were analysed by GC-MS (HP6890s/HP5973 GC/MS, Perkin-Elmer, Norwalk, USA).

### 2.3. Photocatalytic degradation experiments

The photocatalytic degradation experiments were carried out in a homemade photocatalytic reactor. The experimental set-up is shown in figure 1. A high-pressure mercury lamp was used as a light (250 W) source, the distance between the reactor and the light was 20 cm, and the reactor was passed through the condensate to ensure that the entire reaction took place under a constant temperature.

The DBP aqueous solution (100 ml) was placed in the photocatalytic reactor, and then the appropriate amount of Fe<sub>2</sub>O<sub>3</sub> powder and a certain volume of 30% H<sub>2</sub>O<sub>2</sub> were added to conduct the photocatalytic degradation process. The photocatalytic degradation process of DBP over  $\alpha$ -Fe<sub>2</sub>O<sub>3</sub> was carried out by changing the amount of Fe<sub>2</sub>O<sub>3</sub>, H<sub>2</sub>O<sub>2</sub> content, pH and initial concentration of DBP.

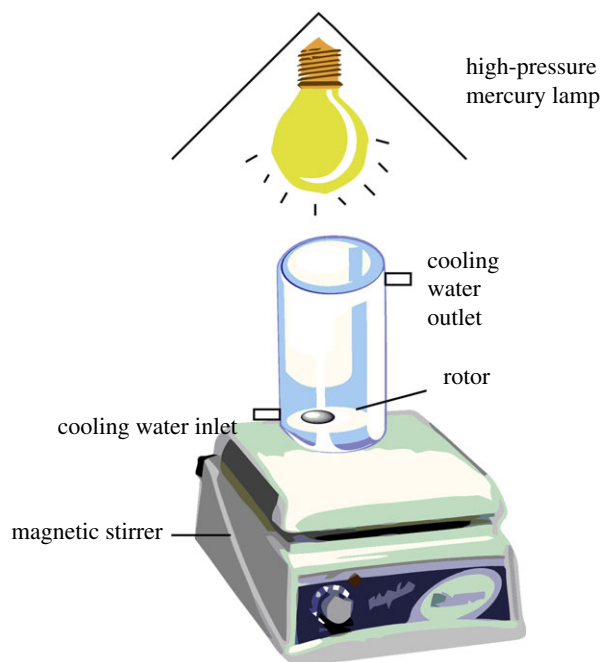


**Figure 1.** Reactor of photocatalysis for DBP.

## 3. Results and discussion

### 3.1. Establishment of the standard curve

The UV–visible spectra of the different concentrations of DBP solution are shown in electronic supplementary material, figure S1. The scanning range was 190–350 nm. The characteristic absorption wavelength of DBP was 230 nm, so that wavelength was selected. The relationship between the mass concentration of DBP solution and the absorbance is shown in electronic supplementary material, figure S2. From the standard curve, the absorbance value at the characteristic absorption wavelength showed a good linear relationship in the DBP solubility range, and the following regression equation was obtained from the standard curve:

$$A = 0.023c + 0.003 \quad R^2 = 0.99, \quad (3.1)$$

where  $A$  is the absorbance and  $c$  is the mass concentration of DBP solution. According to the standard curve, the relationship between the mass concentration and the absorbance was in accordance with the Lambert–Beer rule. Therefore, the degradation efficiency in this concentration range could be expressed by the following formula:

$$K = \frac{A_0 - A_t}{A_0} \times 100\%, \quad (3.2)$$

where  $K$  is the degradation rate,  $A_0$  is the absorbance of the initial solution and  $A_t$  is the absorbance of the solution at time  $t$ .

### 3.2. Effect of $\alpha$ -Fe<sub>2</sub>O<sub>3</sub> particles with different morphology on degradation of dibutyl phthalate

The morphology of  $\alpha$ -Fe<sub>2</sub>O<sub>3</sub> particles is an important factor affecting degradation processes, so it is necessary to explore the effect of  $\alpha$ -Fe<sub>2</sub>O<sub>3</sub> particles with different morphology on degradation of DBP. Figure 2 shows the photocatalytic activity of  $\alpha$ -Fe<sub>2</sub>O<sub>3</sub> with different morphologies for the degradation of DBP. It could be clearly seen that the degradation efficiency varied with  $\alpha$ -Fe<sub>2</sub>O<sub>3</sub> morphology. Among them,  $\alpha$ -Fe<sub>2</sub>O<sub>3</sub> nanoparticles with hollow morphology had the highest degradation efficiency. The possible reason was that the structure of hollow  $\alpha$ -Fe<sub>2</sub>O<sub>3</sub> nanoparticles could produce more hydroxyl radicals ( $\bullet$ OH). In addition, the dispersion of hollow  $\alpha$ -Fe<sub>2</sub>O<sub>3</sub> nanoparticles and the specific surface area were larger than those of other forms of nanoparticles, so the most effective reaction area was obtained. Based on the results shown in figure 2, the hollow morphology was optimal and selected for further studies.

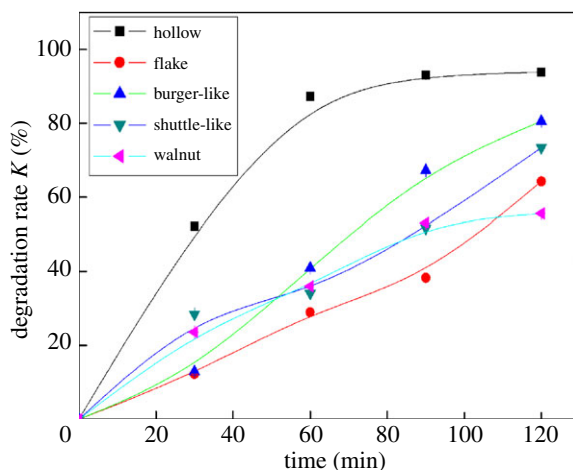


**Figure 2.** Effect of different morphologies of  $\text{Fe}_2\text{O}_3$  on the degradation efficiency of DBP ( $\text{Fe}_2\text{O}_3$ , 30 mg; 30%  $\text{H}_2\text{O}_2$ , 50  $\mu\text{l}$ ; pH = 6.5; temperature, 25°C).

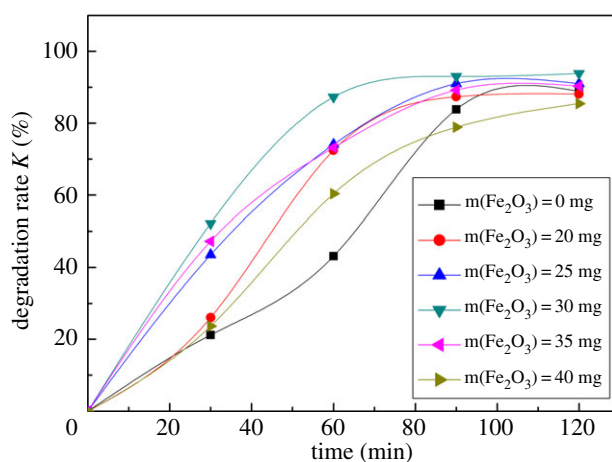


**Figure 3.** Effect of  $\text{Fe}_2\text{O}_3$  content on the degradation efficiency of DBP (13 mg  $\text{l}^{-1}$  DBP, 100 ml; pH = 6.5; temperature, 25°C).

### 3.3. Effect of $\alpha\text{-Fe}_2\text{O}_3$ dosage on the degradation of dibutyl phthalate

The catalyst dosage is also an important factor affecting degradation processes, so it is necessary to explore the effect of  $\alpha\text{-Fe}_2\text{O}_3$  dosage on the degradation efficiency of DBP. To determine the optimal dosage, various amounts of  $\alpha\text{-Fe}_2\text{O}_3$  nanoparticles were tested. Figure 3 shows the degradation of DBP with  $\alpha\text{-Fe}_2\text{O}_3$  dosage. As seen, the degradation efficiency of DBP solution was the highest when the amount of  $\text{Fe}_2\text{O}_3$  was 30 mg/100 ml. This phenomenon was explained as follows. When the effective area of the photocatalytic reaction increased, the amount of photo-generated electron-hole pairs and hydroxyl radicals also increased. This indicated that the degradation rate of DBP was strongly influenced by the number of active sites and photon absorption ability of the  $\alpha\text{-Fe}_2\text{O}_3$  nanoparticles. However, when the amount of the  $\alpha\text{-Fe}_2\text{O}_3$  nanoparticles was too much, the propagation of the incident light in the reaction solution was hindered. At this moment, the light scattering effect increased so that the light transmittance reduced, which affected the photocatalytic degradation efficiency. Based on the results shown in figure 3, the optimal dosage was 30 mg/100 ml.

### 3.4. Effect of $\text{H}_2\text{O}_2$ content on degradation of dibutyl phthalate

As is well known,  $\text{H}_2\text{O}_2$  can be photolysed to produce hydroxyl radical group under light irradiation, the reaction being described as follows:



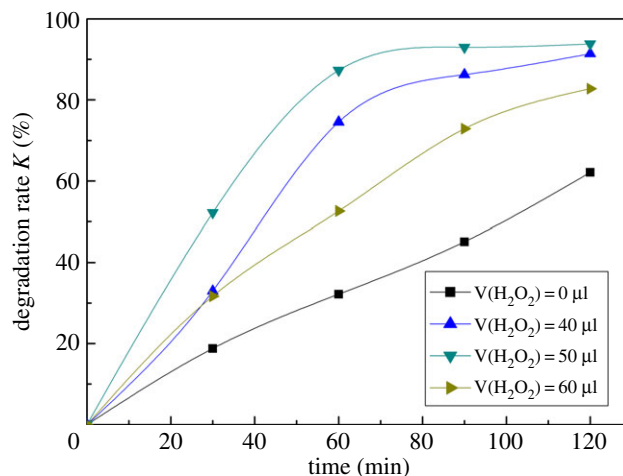
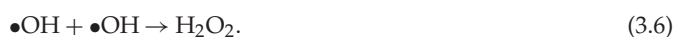


**Figure 4.** Effect of H<sub>2</sub>O<sub>2</sub> content on the degradation efficiency of DBP (13 mg l<sup>-1</sup> DBP, 100 ml; Fe<sub>2</sub>O<sub>3</sub>, 30 mg; pH = 6.5; temperature, 25°C).

The hydroxyl radical group plays a critical role in the degradation process of organics: it can be involved in hydroxyl substitution reaction, dehydrogenation reaction or electron transfer reaction, leading to sensitization and degradation of organics.

Figure 4 shows the effect of H<sub>2</sub>O<sub>2</sub> content on the degradation efficiency of DBP. As seen in figure 4, the degradation efficiency of DBP solution was the highest when H<sub>2</sub>O<sub>2</sub> content was 50 µl. In the photocatalytic reaction system, the addition of H<sub>2</sub>O<sub>2</sub> can increase the rate of hydroxyl radical formation. At the same time, H<sub>2</sub>O<sub>2</sub> is also an electron capture agent that can inhibit the complex effects of photo-generated electron-hole pairs. So the addition of H<sub>2</sub>O<sub>2</sub> could accelerate the photocatalytic degradation efficiency of DBP. When the amount of H<sub>2</sub>O<sub>2</sub> was less, the •OH produced in the reaction system was less, so the degradation efficiency was low. With the increase of H<sub>2</sub>O<sub>2</sub> content, the formation rate of •OH in the system also increased, so the photocatalytic degradation efficiency was obviously improved. However, when the H<sub>2</sub>O<sub>2</sub> addition exceeded the critical value, the generation of •OH was inhibited because excessive H<sub>2</sub>O<sub>2</sub> had a capture effect on •OH, resulting in a decrease in degradation efficiency. The reaction is described as follows:



According to the results shown in figure 4, the optimal 30% H<sub>2</sub>O content was 50 µl.

### 3.5. Effect of solution pH on degradation of dibutyl phthalate

For the multi-phase photocatalytic reaction of semiconductors, the pH value of the solution is an important factor affecting the kinetics of catalytic reaction. Figure 5 shows the effect of pH on the degradation of DBP. The photocatalytic degradation rate of DBP in Fe<sub>2</sub>O<sub>3</sub>/H<sub>2</sub>O<sub>2</sub>/UV system was the fastest under neutral condition. The main mechanism is described as follows: (1) different pH values can change the charge properties of the catalyst, especially the oxide semiconductor, so it can affect the adsorption behaviour of organic molecules on the catalyst surface; (2) H<sup>+</sup> or OH<sup>-</sup> in the solution can combine with the photo-generated charge to produce highly active species; and (3) change of pH may lead to change of some organic structure, thereby it can change the ease of catalytic oxidation.

The degradation efficiency of DBP was lower under acidic condition, and the photocatalytic degradation efficiency was the lowest under alkaline condition. This might be related to the stability of DBP at different pH conditions and the effect of the products obtained by photocatalytic degradation of DBP. Under acidic condition, DBP was more susceptible to oxidative degradation to produce organic acids such as benzoic acid, carboxylic acid and CO<sub>2</sub>, which reduces the reaction rate of the whole degradation process. Under alkaline condition, H<sub>2</sub>O<sub>2</sub> was very unstable and easily decomposed into H<sub>2</sub>O and O<sub>2</sub>, so that the H<sub>2</sub>O<sub>2</sub> content became low, which might affect the formation of •OH. So the photocatalytic degradation rate became slower. Based on the results shown in figure 5, the optimal pH was that of neutral condition.

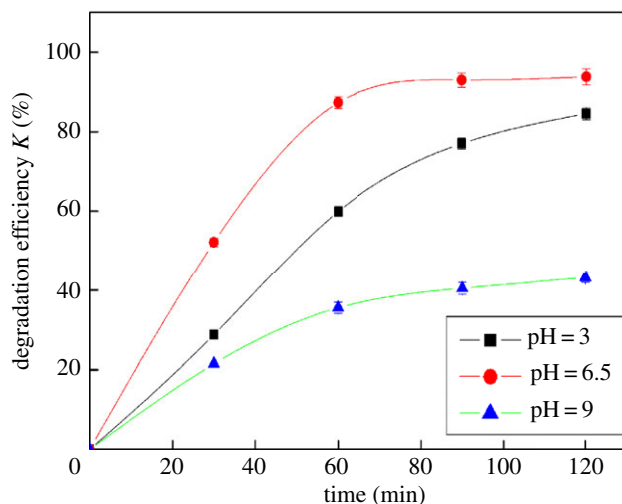


**Figure 5.** Effect of pH on the degradation of DBP ( $13 \text{ mg l}^{-1}$  DBP, 100 ml; 30%  $\text{H}_2\text{O}_2$ , 50  $\mu\text{l}$ ;  $\text{Fe}_2\text{O}_3$ , 30 mg; temperature,  $25^\circ\text{C}$ ).

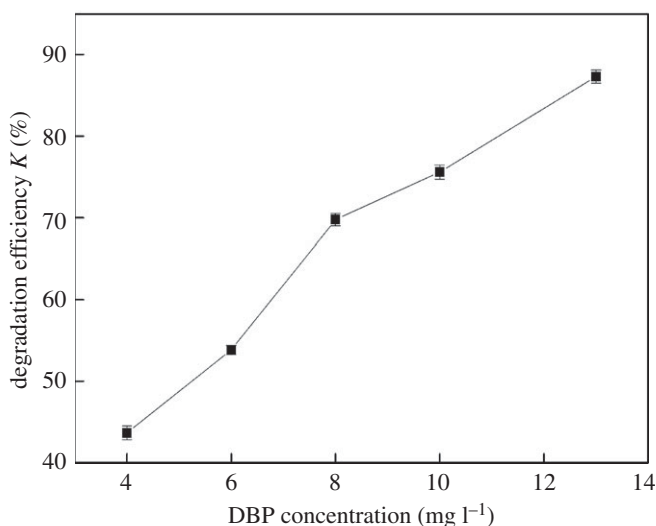


**Figure 6.** Effect of different initial concentration on the degradation efficiency ( $13 \text{ mg l}^{-1}$  DBP, 100 ml; 30%  $\text{H}_2\text{O}_2$ , 50  $\mu\text{l}$ ;  $\text{Fe}_2\text{O}_3$ , 30 mg; temperature,  $25^\circ\text{C}$ ).

### 3.6. Effect of initial dibutyl phthalate concentration on degradation of dibutyl phthalate

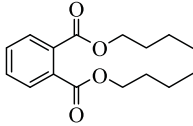
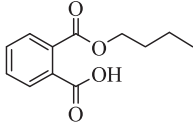
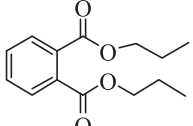
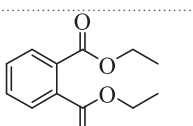
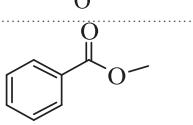
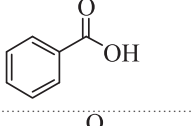
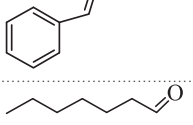
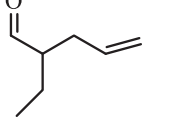
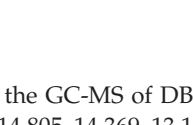
In general, the photocatalytic degradation of organics involves the processes of the charge transfer of organics and reactive groups (electron-hole pairs,  $\bullet\text{OH}$ , etc.) that take place on the surface of the catalyst. Therefore, the initial concentration of organics has also an influence on the photocatalytic degradation efficiency.

Figure 6 shows the effect of different initial concentration on the degradation efficiency of DBP. The degradation rate increased with the initial concentration in the range of solubility of DBP. When the initial concentration was  $13 \text{ mg l}^{-1}$ , the photocatalytic degradation efficiency was the highest. As the maximal solubility of DBP in water was  $13 \text{ mg l}^{-1}$ ,  $13 \text{ mg l}^{-1}$  of DBP solution was selected for photocatalytic degradation in this study.

### 3.7. Photocatalytic degradation process and mechanism of dibutyl phthalate

GC-MS not only can determine the molecular structure of a compound, and but also accurately determine the relative molecular weight of unknown components. In order to further study the photocatalytic degradation process and mechanism of DBP under high-pressure mercury lamp irradiation for 2 h and 12 h, the corresponding degradation intermediates of DBP were analysed by GC-MS.

**Table 1.** The main intermediate photocatalytic degradation products of DBP.

retention time (min)	products	structure	molecular weight
14.965	dibutyl phthalate		278
14.805	2-(butoxycarbonyl)benzoic acid		222
14.369	dipropyl phthalate		250
13.133	diethyl phthalate		222
12.673	methyl benzoate		136
12.211	benzoic acid		122
10.936	benzaldehyde		106
10.316	heptanal		114
10.022	2-ethylpent-4-enal		112

Electronic supplementary material, figures S3–S13, show the GC-MS of DBP and main degradation intermediates. The corresponding retention time was 14.965, 14.805, 14.369, 13.133, 12.673, 12.211, 10.936, 10.316, 10.022 and 7.266 min, respectively. The analytic results are listed in table 1. Based on these results, the probable photocatalytic degradation pathway of DBP is shown in figure 7, and the probable reaction process and degradation mechanism were proposed as follows.

In the process of reaction, the electron-hole pairs generated from the excitation of photocatalyst  $\alpha$ -Fe<sub>2</sub>O<sub>3</sub> nanoparticles were transferred to the surface of the catalyst and combined with OH<sup>-</sup>, O<sub>2</sub>, H<sub>2</sub>O, etc. and adsorbed on the surface of the catalyst with the occurrence of energy and charge exchange, showing a strong oxidizing ability of hydroxyl radicals •OH, etc. First, the ester of the CO bond and the carbon chain of DBP in the solution were attacked by •OH to produce mono-butyl phthalate, phthalate and alkane moiety. Second, the carbon chain from different locations might be broken and the main products such as diethyl phthalate and dipropyl phthalate appeared. Under the action of •OH, phthalic acid and methyl benzoate formed benzoic acid. The C–O bonds in the carboxylic acid and carboxyl group were fractured and oxidized to generate benzaldehyde and then benzene formaldehyde was attacked by •OH, forming the heptaldehyde and 2-ethyl-4-pentenal. It could be seen that there were many possibilities for the ring-opening reaction of the benzene ring. The active group •OH attacked the terminal alkene group, resulting in valeraldehyde. Finally, CO<sub>2</sub> and H<sub>2</sub>O could be produced by •OH.

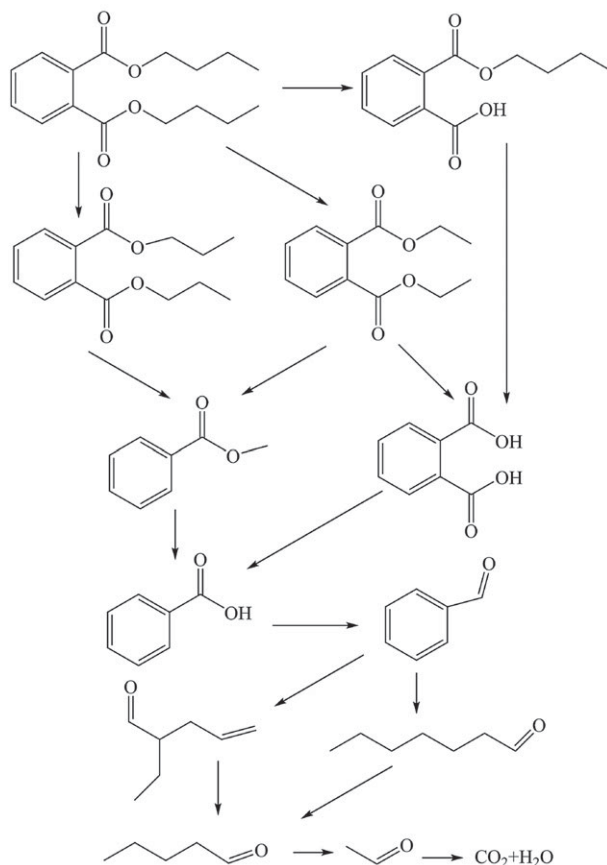


**Figure 7.** Photocatalytic degradation mechanism of DBP.

## 4. Conclusion

In this study,  $\alpha\text{-Fe}_2\text{O}_3/\text{H}_2\text{O}_2/\text{UV}$  was used as the photocatalytic degradation system of DBP. The optimum experimental conditions were obtained, and the maximum degradation efficiency could reach 94% when the hollow  $\alpha\text{-Fe}_2\text{O}_3$  dosage, 30%  $\text{H}_2\text{O}_2$  content, pH value and initial DBP concentration were  $300\text{ mg l}^{-1}$ ,  $50\ \mu\text{l}$ , 6.5 and  $13\text{ mg l}^{-1}$ , respectively. DBP could be degraded by the attack of active hydroxyl radicals, producing the corresponding intermediates, such as monobutyl phthalate, diethyl phthalate, methyl benzoate, benzoic acid, benzaldehyde, heptaldehyde, 2-ethyl-4-pentenal, during the reaction for 2 h. The DBP and its intermediates were almost completely degraded to mineralize to  $\text{CO}_2$  and  $\text{H}_2\text{O}$ . These results illustrated that hollow  $\alpha\text{-Fe}_2\text{O}_3$  nanoparticles have great potential as catalyst to process more organic pollutants in the environment and provide technical support for the further study of the photocatalytic degradation of other organic pollutants.

**Data accessibility.** This article does not contain any additional data.

**Authors' contributions.** J.H. and G.Q. designed the study. Y.L. and N.S. prepared all samples for analysis. Y.L., N.S. and S.L. collected and analysed the data. Y.L. and N.S. interpreted the results and wrote the manuscript. All authors gave final approval for publication.

**Competing interests.** The authors declare no competing interests.

**Funding.** Financial support came from the HI-Tech Research and Development Program (863) of China (2012AA030314-2), and Science and Fundamental Research Funds for the Central Universities (N160504001).

## References

- Castle L, Mercer AJ, Startin JR, Gilbert J. 1998 Migration from plasticized films into foods 3. Migration of phthalate, sebacate, citrate and phosphate esters from films used for retail food packaging. *Food Addit. Contam.* **5**, 9–20. (doi:10.1080/02652038809373657)
- Wams T. 1987 Diethyl hexylphthalate as an environmental contaminant—a review. *Sci. Total Environ.* **66**, 1–16. (doi:10.1016/0048-9697(87)90072-6)
- Fang CR, Yao J, Zheng YG, Jiang CJ, Hu LF, Wu YY, Shen DS. 2010 Diethylhexylphthalate as an



- environmental contaminant—a review. *Int. Biodeter. Biodegr.* **64**, 442–446. (doi:10.1016/j.ibiod.2010.04.010)
4. Bajt O, Mailhot G, Bolte M. 2001 Degradation of dibutyl phthalate by homogeneous photocatalysis with Fe (III) in aqueous solution. *Appl. Catal. B* **33**, 239–248. (doi:10.1016/S0926-3373(01)00179-5)
  5. Fankhauser-Noti A, Grob K. 2007 Blank problems in trace analysis of diethylhexyl and dibutyl phthalate: investigation of the sources, tips and tricks. *Anal. Chim. Acta* **582**, 353–360. (doi:10.1016/j.aca.2006.09.012)
  6. Li LS, Zhu WP, Chen L, Zhang PY, Chen ZY. 2005 Photocatalytic ozonation of dibutyl phthalate over TiO<sub>2</sub> film. *J. Photochem. Photobiol. B* **175**, 172–177. (doi:10.1016/j.jphotochem.2005.01.020)
  7. Sandhwar VK, Prasad B. 2017 Comparative study of electrochemical oxidation and electrochemical Fenton processes for simultaneous degradation of phthalic and para-toluic acids from aqueous medium. *J. Mol. Liq.* **243**, 519–532. (doi:10.1016/j.molliq.2017.08.016)
  8. Yan XL, Yang YL, Wang C, Hu XY, Zhou, M, Komarmeni S. 2016 Surfactant-assisted synthesis of ZIF-8 nanocrystals for phthalic acid adsorption. *J. Sol-Gel. Sci. Technol.* **80**, 523–530. (doi:10.1007/s10971-016-4138-5)
  9. Wang JL, Lou YY, Xu C, Song S, Liu WP. 2016 Magnetic lanthanide oxide catalysts: an application and comparison in the heterogeneous catalytic ozonation of diethyl phthalate in aqueous solution. *Sep. Purif. Technol.* **159**, 57–67. (doi:10.1016/j.seppur.2015.12.031)
  10. Tang WJ, Zhang LS, Fang Y, Zhou Y, Ye BC. 2016 Biodegradation of phthalate esters by newly isolated *Rhizobium* sp. LMB-1 and its biochemical pathway of di-*n*-butyl phthalate. *J. Appl. Microbiol.* **121**, 177–186. (doi:10.1111/jam.13123)
  11. Khataee AR, Pons MN, Brown R, Zahraa O. 2009 Photocatalytic degradation of three azo dyes using immobilized TiO<sub>2</sub> nanoparticles on glass plates activated by UV light irradiation: influence of dye molecular structure. *J. Hazard. Mater.* **168**, 451–457. (doi:10.1016/j.jhazmat.2009.02.052)
  12. Petronella F, Truppi A, Ingrosso C, Placido T, Striccooli M, Curri ML, Agostiano A, Comparelli R. 2017 Nanocomposite materials for photocatalytic degradation of pollutants. *Catal. Today* **281**, 85–100. (doi:10.1016/j.cattod.2016.05.048)
  13. Ahmed S, Rasul MG, Martens WN, Hashib MA. 2010 Heterogeneous photocatalytic degradation of phenols in wastewater: a review on current status and developments. *Desalination* **261**, 3–18. (doi:10.1016/j.desal.2010.04.062)
  14. Bhatkhande DS, Pangarkar VG, Beenackers AA. 2002 Photocatalytic degradation for environmental applications—a review. *J. Chem. Technol. Biotechnol.* **77**, 102–116. (doi:10.1002/jctb.532)
  15. Liu S, Hu QK, Qiu JL, Wang FX, Zhu F, Wei CH, Zhou NB, Ouyang GF. 2017 Enhanced photocatalytic degradation of environmental pollutants under visible irradiation by a composite coating. *Environ. Sci. Technol.* **51**, 5137–5145. (doi:10.1021/acs.est.7b00350)
  16. Barroso M, Cowan AJ, Pendlebury SR, Gratzel M, Klug DR, Durrant JR. 2011 The role of cobalt phosphate in enhancing the photocatalytic activity of  $\alpha$ -Fe<sub>2</sub>O<sub>3</sub> toward water oxidation. *J. Am. Chem. Soc.* **133**, 14 868–14 871. (doi:10.1021/ja205325v)
  17. Li LL, Chu Y, Liu Y, Dong LH. 2007 Template-free synthesis and photocatalytic properties of novel Fe<sub>2</sub>O<sub>3</sub> hollow spheres. *J. Phys. Chem. C* **111**, 2123–2127. (doi:10.1021/jp066664y)
  18. Cao SW, Zhu YJ. 2008 Hierarchically nanostructured  $\alpha$ -Fe<sub>2</sub>O<sub>3</sub> hollow spheres: preparation, growth mechanism, photocatalytic property, and application in water treatment. *J. Phys. Chem. C* **112**, 6253–6257. (doi:10.1021/jp8000465)
  19. Karthikeyan K, Amaresh S, Lee SN, Aravindan V, Lee YS. 2014 Fluorine-doped Fe<sub>2</sub>O<sub>3</sub> as high energy density electroactive material for hybrid supercapacitor applications. *Chem. Asian J.* **9**, 852–857. (doi:10.1002/asia.201301289)
  20. Iturrondobeitia A, Gofii A, Orue I, Rojo T. 2015 Effect of carbon coating on the physicochemical and electrochemical properties of Fe<sub>2</sub>O<sub>3</sub> nanoparticles for anode application in high performance lithium ion batteries. *Inorg. Chem.* **54**, 5239–5248. (doi:10.1021/acs.inorgchem.5b00203)
  21. Gu S, Lou Z, Li L, Shen GZ. 2016 Fabrication of flexible reduced graphene oxide/Fe<sub>2</sub>O<sub>3</sub> hollow nanospheres based on-chip micro-supercapacitors for integrated photodetecting applications. *Nano Res.* **9**, 424–434. (doi:10.1007/s12274-015-0923-7)
  22. Humayun M, Li Z, Sun L, Zhang XL, Raziq F, Zada A, Qu Y, Jing LQ. 2016 Coupling of nanocrystalline anatase TiO<sub>2</sub> to porous nanosized LaFeO<sub>3</sub> for efficient visible-light photocatalytic degradation of pollutants. *Nanomaterials* **6**, 22. (doi:10.3390/nano6010022)
  23. Vaiano V, Sacco O, Sannino D, Ciambelli P, Longo S, Venditto V, Guerra G. 2014 N-doped TiO<sub>2</sub>/s-PS aerogels for photocatalytic degradation of organic dyes in wastewater under visible light irradiation. *J. Chem. Technol. Biotechnol.* **89**, 1175–1181. (doi:10.1002/jctb.4372)
  24. Luo X, Deng F, Min L, Luo SL, Guo B, Zeng BG, Au C. 2013 Facile one-step synthesis of inorganic-framework molecularly imprinted TiO<sub>2</sub>/WO<sub>3</sub> nanocomposite and its molecular recognitive photocatalytic degradation of target contaminant. *Environ. Sci. Technol.* **47**, 7404–7412. (doi:10.1021/es4013596)
  25. Matsumoto YJ. 1996 Energy positions of oxide semiconductors and photocatalysis with iron complex oxides. *Solid State Chem.* **126**, 227–234. (doi:10.1006/jssc.1996.0333)
  26. Hu JS, Sun N, Li S, Qin GW. 2015 Controllable preparation of  $\alpha$ -Fe<sub>2</sub>O<sub>3</sub> particles with different morphology. *J. Northeast. Univ.* **36**, 1260–1264.